Correction of bias of the HadGEM2-CC climate model of the Met Office Hadley Centre (MOHC) for the specific humidity climate variable in the Northwest Region of Madagascar and observation of climate change

MAXWELL Djaffard[1], DONA Victorien Bruno[1], RAKOTOVELO Geoslin[1], RATIARISON Adolphe Andriamanga[2]

[1]*Laboratory of Applied Physics and Renewable Energies, Mahajanga University, Madagascar*
[2]*Laboratory of Atmospheric, Climate and Ocean Dynamics, University of Antananarivo, Madagascar*

ABSTRACT

This article presents the study of specific humidities in the North-West region of Madagascar, delimited by latitudes from -15 ° to -18 ° and longitudes from 44 ° to 48. The study of the evolution of annual averages of specific humidities at 700 and 850 hPa levels showed the absence of significant trend based on the Mann Kendall test.
The area can be subdivided into 5 regions with respect to the specific humidity at the 700 hPa level and 2 regions relative to the specific humidity at the 850 hPa level.
The bias correction of Hadley Center's HadGEM2-CC climate model by the debinding method, the quantile-quantile method and the delta method was performed for each region. The results reveal that one method of bias correction can be adapted to one region but not for another.

Keyword: *humidity, climatological mean, anomaly, trend, Mann-Kendall test, Principal Component Analysis, climate model, debinding method, quantile-quantile method, delta method, RCP4.5, RCP8.5*

1. INTRODUCTION

Comparison of the mean of climate simulations with that of observations for a given parameter over a given period and space generally shows a good similarity. However the agreement is not perfect because there are not only systematic errors on the averages, but also some extremes are not reproduced very well.
To make the statistical distribution of the daily data as close as possible to the distribution observed at each point, it is necessary to correct bias to minimise the error between the observation made and the climate model. **Figure** 1 represents the study area located in northwestern Madagascar. It is delimited by latitudes -15 ° to -18 ° and longitudes 44 ° to 48 °.

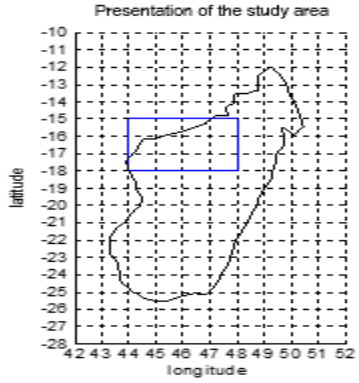

Figure 1: Representation of the study area

2. METHODOLOGIES

2.1 Data

Observation data : specific humidity data 1979-2016 from NOAA
Projection data : specific humidity projection data from 2006 to 2054 for each RCP4.5 and RCP8.5 scenario from CERFACS.
Historical data : Historical specific humidity data from the HadGEM2-CC model of the Met Office Hadley Center (MOHC) from 1979 to 2005 under the RCP4.5 and RCP8.5 scenarios from CERFACS.

2.2 Methods

The methodology applied is to use:

- the **Mann-Kendall test** to detect the presence of trends within a time series in the absence of any seasonality or other cycles. The calculated statistic is defined by:

$$S=\sum_{i=1}^{n-1}\sum_{j=i+1}^{n}\operatorname{sgn}\left[\left(y_j-y_i\right)\left(x_j-x_i\right)\right] \text{ where } \operatorname{sgn}(\mathrm{X})=\begin{cases}+1 \text{ if } X>0\\ 0 \text{ if } X=0\\ -1 \text{ if } X<0\end{cases}$$

Mann (1945) and Kendall (1975) demonstrated that:

$$\begin{cases}E(S)=0\\ Var(S)=\dfrac{n(n-1)(2n+5)}{18}\end{cases}$$

If there are ex-aequo in the series, the variance of S is corrected as follows:

$$Var(S)=\frac{1}{18}\left[n(n-1)(2n+5)-\sum_{p=1}^{g}t_p\,(p-1)(2p+5)\right] \text{ where } t_p \text{ is the number of equalities involving } p \text{ values}$$

As soon as the sample contains about a dozen data, the law of Z-test statistics can be approached by a centered-reduced gaussian.

$$Z=\begin{cases}\dfrac{S-1}{(Var(S))^{\frac{1}{2}}} & \text{if S>0}\\ 0 \text{ si S=0}\\ \dfrac{S+1}{(Var(S))^{\frac{1}{2}}} & \text{if S<0}\end{cases}$$

If we have a sequence of observations $x_1, x_2, \ldots, x_n$ for which we make the two hypotheses:

$$\begin{cases}\text{Hypothesis null } H_0\text{: observations } x_i \text{ are randomly ordered, no trend}\\ \text{Alternative Hypothesis } H_1\text{: Observations } x_i \text{ shows increasing or decreasing trend}\end{cases}$$

The trend of the observation sequence is statistically significant when the p-value of the test is less than 5%. **[1]**

- **Normalized Principal Components Analysis**, which is a factorial dimension reduction method for the statistical exploration of complex quantitative data. This method is widely used in the analysis of climatological data. **[2], [3], [4], [5]**
  - For two statistical series $k=(x_k, n_k)$ and $h=(x_h, n_h)$ of the same size n with a time depth of several years, the linear correlation coefficient is given by:

$$r(k,h)=\frac{1}{n}\sum_{i=1}^{n}\left(\frac{x_{ik}-\bar{x}_k}{s_k}\right)\left(\frac{x_{ih}-\bar{x}_h}{s_h}\right) \text{ where } \begin{cases}\bar{x}_k\text{: mean of k}\\ s_k\text{: standard deviation of k}\end{cases} \begin{cases}\bar{x}_h\text{: mean of h}\\ s_h\text{: standard deviation of h}\end{cases}$$

- Data matrix:

Iinitial data table

$$T = \begin{pmatrix} v_{11} & v_{21} & \cdot & \cdot & \cdot & v_{1(p-1)} & v_{1p} \\ v_{21} & v_{22} & \cdot & \cdot & \cdot & v_{2(p-1)} & v_{2p} \\ \cdot & \cdot & \cdot & \cdot & \cdot & \cdot & \cdot \\ \cdot & \cdot & \cdot & \cdot & \cdot & \cdot & \cdot \\ \cdot & \cdot & \cdot & \cdot & \cdot & \cdot & \cdot \\ v_{(n-1)1} & v_{(n-1)2} & \cdot & \cdot & \cdot & v_{(n-1)(p-1)} & v_{(n-1)p} \\ v_{n1} & v_{n2} & \cdot & \cdot & \cdot & v_{n(p-1)} & v_{np} \end{pmatrix}$$

Cloud point center of gravity

$$G = \begin{pmatrix} x_{G1} = \dfrac{\sum_{i=1}^{n} v_{i1}}{n} \\ \cdot \\ \cdot \\ \cdot \\ x_{Gp} = \dfrac{\sum_{i=1}^{n} v_{ip}}{n} \end{pmatrix}$$

Choosing G as the origin leads to the reduced data center table

$$T_{cr} = \begin{pmatrix} \dfrac{v_{11} - x_{G11}}{s_1} & \dfrac{v_{21} - x_{G21}}{s_2} & \cdot \cdot \cdot & \dfrac{v_{1(p-1)} - x_{G1(p-1)}}{s_{(p-1)}} & \dfrac{v_{1p} - x_{G1p}}{s_p} \\ \dfrac{v_{21} - x_{G21}}{s_1} & \dfrac{v_{22} - x_{G22}}{s_2} & \cdot \cdot \cdot & \dfrac{v_{2(p-1)} - x_{G2(p-1)}}{s_{(p-1)}} & \dfrac{v_{2p} - x_{G2p}}{s_p} \\ \cdot & \cdot & \cdot \cdot \cdot & \cdot & \cdot \\ \cdot & \cdot & \cdot \cdot \cdot & \cdot & \cdot \\ \cdot & \cdot & \cdot \cdot \cdot & \cdot & \cdot \\ \dfrac{v_{(n-1)1} - x_{G(n-1)1}}{s_1} & \dfrac{v_{(n-1)2} - x_{G(n-1)2}}{s_2} & \cdot \cdot \cdot & \dfrac{v_{(n-1)(p-1)} - x_{G(n-1)(p-1)}}{s_{(p-1)}} & \dfrac{v_{(n-1)p} - x_{G(n-1)p}}{s_p} \\ \dfrac{v_{n1} - x_{Gn1}}{s_1} & \dfrac{v_{n2} - x_{Gn2}}{s_2} & \cdot \cdot \cdot & \dfrac{v_{n(p-1)} - x_{Gn(p-1)}}{s_{(p-1)}} & \dfrac{v_{np} - x_{Gnp}}{s_p} \end{pmatrix}$$

Reduced centered coordinates of the individual u_i :

$$X_{cri} = \begin{pmatrix} \dfrac{v_{i1} - x_{Gi1}}{s_1} \\ - \\ - \\ - \\ \dfrac{v_{ip} - x_{Gip}}{s_p} \end{pmatrix}$$

Total inertia of the cloud of individuals :

$$I_G = \frac{1}{n}\sum_{i=1}^{n}\sum_{j=1}^{p}\left(\frac{v_{ij} - x_{Gij}}{s_j}\right)^2 = \sum_{j=1}^{p}\left(\frac{1}{n}\sum_{i=1}^{n}\left(\frac{v_{ij} - x_{Gij}}{s_j}\right)^2\right) = \sum_{j=1}^{p}\left(\mathrm{r}\left(v_{ij}\right)\right)$$

Covariance matrix:

$$R = \begin{pmatrix} r(v_{11}) & r(v_{12}) & \cdots & r(v_{1(p-1)}) & r(v_{1p}) \\ r(v_{21}) & r(v_{22}) & \cdots & r(v_{2(p-1)}) & r(v_{2p}) \\ \vdots & \vdots & \cdots & \vdots & \vdots \\ r(v_{(p-1)1}) & r(v_{(p-1)2}) & \cdots & r(v_{(p-1)(p-1)}) & r(v_{(p-1)p}) \\ r(v_{p1}) & r(v_{p2}) & \cdots & r(v_{p(p-1)}) & r(v_{pp}) \end{pmatrix} = \begin{pmatrix} 1 & \cdots & & & \\ \cdots & 1 & \cdots & & \\ & \cdots & 1 & \cdots & \\ & & \cdots & 1 & \cdots \\ & & & \cdots & 1 \end{pmatrix}$$

$$so\ trace(R) = p = I_G$$

- Eigenvalues and eigenvectors :

$$T_{cr}(V) = \lambda V \text{ où } \begin{cases} \lambda \text{ valeur propre} \\ V \text{ vecteur propre} \end{cases}$$

Axes Δ_i passing through G and minimum inertia have for vector director eigenvectors V_i associated with eigenvaluess λ_i such as

$$I_G = \sum_{i=1}^{p} \lambda_i$$

- Selection of the principal axes to be chosen

$$\sum_{i=1}^{p} \lambda_i = p \Rightarrow \bar{\lambda} = \frac{\sum_{i=1}^{p} \lambda_i}{p} = 1 \text{ therefore we can not consider as significant that the } \lambda_i \geq 1$$

By Kaiser's empirical criterion, by centering and reducing the data, we retain the principal components corresponding to eigenvalues greater than 1. **[6]**

- Quality of representation of an individual u_i on an axis Δ_k

The parameter $cos^2\theta$ is used to characterize the quality of representation (qlt) on an axis**. [6]**

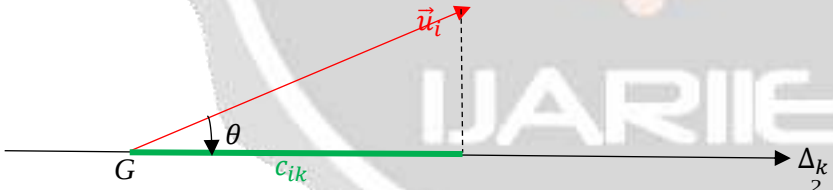

$$qlt_k(u_i) = \cos^2(\theta) = \frac{c_{ik}^2}{\left\|\overrightarrow{Gu_i}\right\|^2}$$

$$\left\|\overrightarrow{Gu_i}\right\|^2 = \sum_{k=1}^{p} c_{ik}^2$$

The closer qlt_i is to 1, the better it is represented.
The closer qlt_i is to 0, the more it is misrepresented. **[7]**

Quality of representation of variables**. [2], [3], [4]**
On a factorial plane defined by two pricipal axes :

- a variable close to the correlation circle is well represented in this plane;
- a variable close to the origin of the correlation circle is poorly represented in this plane.

- the **bias correction** by the debinding method, the delta method and the quantile-quantile method: **[8], [9] [10]**
  - debinding method:

$$\begin{cases} B(x,y) = [Mp(x,y,t)] - [O(x,y,t)] \\ Mfc(x,y,t) = Mf(x,y,t) - B(x,y) \\ Mpc(x,y,t) = Mp(x,y,t) - B(x,y) \end{cases} \text{ with } \begin{cases} \text{B : bias} \\ \text{O: observation} \\ \text{M : model} \\ \text{p : present} \\ \text{f : future} \\ \text{c : corrected} \\ [\ ] : \text{climatological mean} \end{cases}$$

- delta method :

$$\begin{cases} Delta(x,y) = \left[M_f(x,y,t)\right] - \left[M_p(x,y,t)\right] \\ M_{fc}(x,y,t) = O(x,y,t) + Delta(x,y) \end{cases} \text{ with } \begin{cases} O: \text{ observation} \\ \text{M : model} \\ \text{p : present} \\ \text{f : future} \\ \text{c : corrected} \\ [\ ] : \text{climatological mean} \end{cases}$$

- Quantile-quantile method :

The order quantiles of 0.01% to 99.9% of the daily values of the simulation considered and the observations are calculated, taking into account the same learning period.

In a point i of the grid and for each order k of quantile, we calculate the correction coefficient $Corr^k(i)$ given by :

$$Corr^k(i) = \begin{cases} 0 \ si \ Q^k(i) = 0 \\ \dfrac{Q_{obs}{}^k(i)}{Q^k(i)} \ si \ Q^k(i) \neq 0 \end{cases} \text{ with } \begin{cases} Q^k(i): value\ at\ point\ i\ of\ the\ quantile\ simulated\ model\ of\ order\ k \\ Q_{obs}{}^k(i): value\ of\ the\ corresponding\ observation\ quantile \end{cases}$$

For each day j of the period and in a point i of the grid of the observations data, we look for the order k of the model quantile (interpolated) directly inferior to the value of the daily O(j, i) of day j at the point i:

$$k = \begin{cases} 0,999 \text{ if } O(j,i) \geq Q^{0.999}(i) \\ otherwise\ k\ is\ such\ that\ Q^k(i) \leq O(j,i) < Q^{k+1}(i) \end{cases}$$

The corrected value of day j at point i, is given by the formula :

$$M_c(j,i) = O(j,i) * Corr^k(i)$$

3. RESULTS AND DISCUSSIONS

3.1 Climatological mean specific humidities from 1979 to 2016 in the study area

Figure 2 shows the daily and monthly climatological mean curves in the study area. The red and blue curves are respectively the climatological mean climatological of specific humidity on 700 hPa and 850 hPa levels over the study period.

The maximum of the daily climatological mean of specific humidity on 700 hPa level is 5.105 $x10^{-3}$ $kg.kg^{-1}$ (mean specific humidities on 700 hPa level of all January 25) and its minimum is 1.768$x10^{-3}$ $kg.kg^{-1}$ (mean of specific humidities on 700 hPa level of all July 16). **(Figure 2-a)**

The maximum of the monthly climatological mean of specific humidity on 700 hPa level is 4.67 $x10^{-3}$ $kg.kg^{-1}$ (mean specific humidities on 700 hPa level of all the months of February) and its minimum is 1.987$x10^{-3}$ $kg.kg^{-1}$ (mean of specific humidities on 700 hPa level of all the months of July). **(Figure 2-b)**

The maximum of the daily climatological mean of specific humidity on 850 hPa level is 8.209 $x10^{-4}$ $kg.kg^{-1}$ (mean specific humidities on 850 hPa level of all January 18) and its minimum is 0.967 $x10^{-4}$ $kg.kg^{-1}$ (mean of specific humidities on 850 hPa level of all July 27). **(Figure 2-c)**

The maximum of the monthly climatological mean of specific humidity on 850 hPa level is 8.334 x10^{-4} kg.kg^{-1} (mean specific humidities on 850 hPa level of all the months of February) and its minimum is 2.068 x10^{-4} kg.kg^{-1} (mean of specific humidities on 850 hPa level of all the months of July). **(Figure 2-d)**

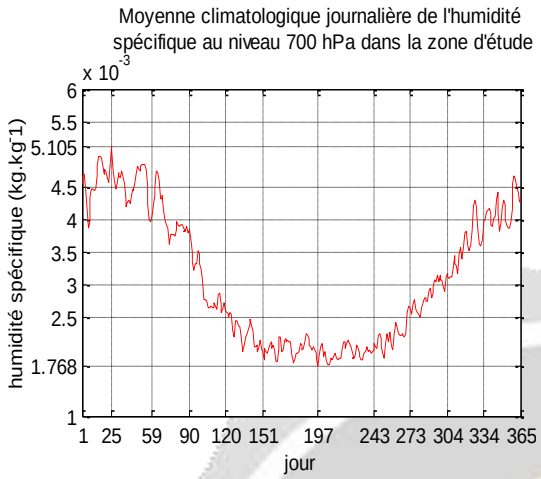

Figure 2-a

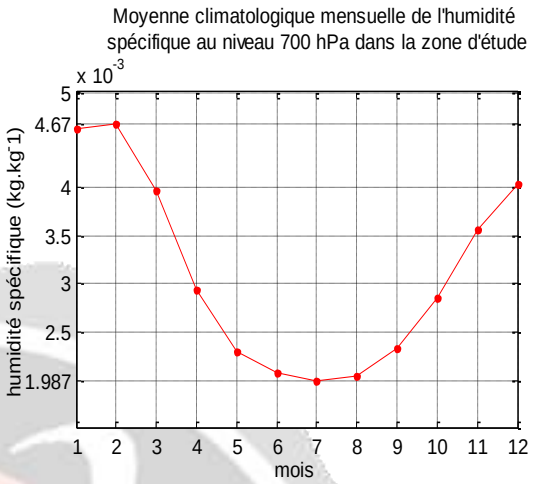

Figure 2-b

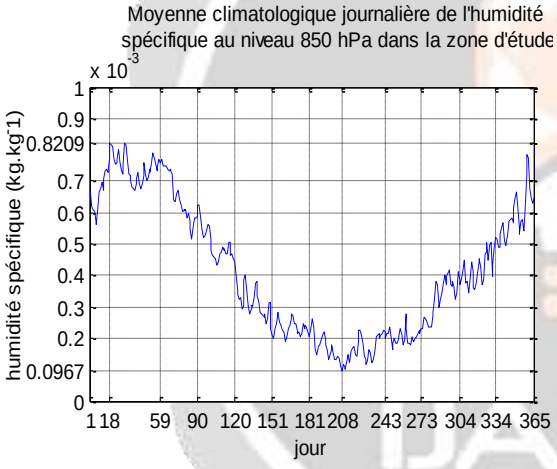

Figure 2-c

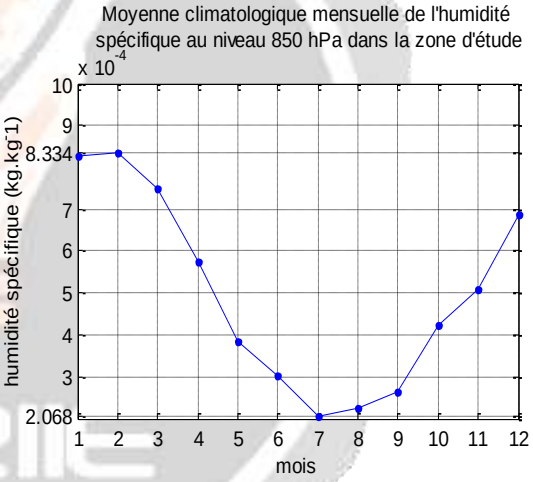

Figure 2-d

Figure 2 : Variation in climatological daily and monthly mean of specific humidities on 850 hPa and 700 hPa levels

3.2 Evolution of annual mean of specific humidities since 1979 to 2016

Figure 3 shows the evolution of the specific humidity annual mean on 700 hPa level (red curve) and on 850 hPa level (blue curves).

The purple line represents the trend for specific humidity on 700 hPa level. Its equation is $y = -0.0000278x + 0.0034466$ where the origin is the year 1979. The slope being negative therefore the specific humidity on 700 hPa level has a downward trend of -2.78x10^{-5} kg.kg^{-1} per year. The Mann Kendall test gives a p-value equal to 0.11318. Since this value is much greater than 0.05, the trend is not significant. (**Figure 3-a**) The black line represents the evolution trend for specific humidity on 850 hPa level from 1979 to 2016, Its equation is $y = -0.0034148 * 10^{-3} x + 0.3164370 * 10^{-3}$. It has a negative slope, so the specific humidity on 850 hPa level also has a downward trend of about -3.41x10^{-6} kg.kg^{-1} per year. The value of the p-value is equal to 0.1591153, which is well above 0,05 : this trend is not significant either. (**Figure 3-b**)

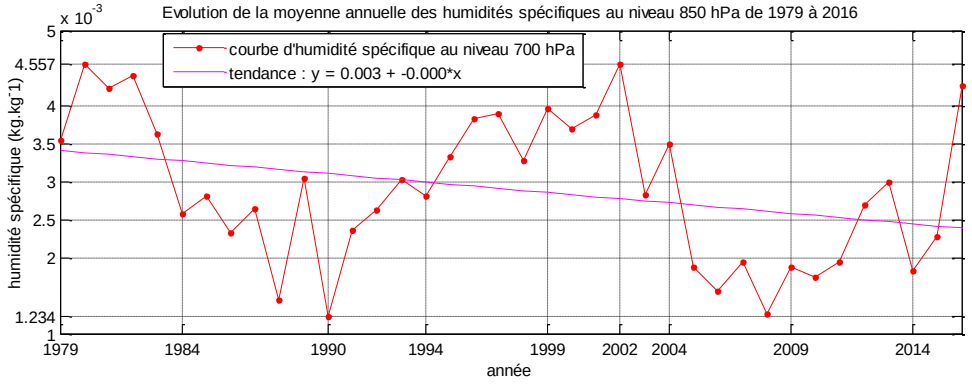

Figure 3-a

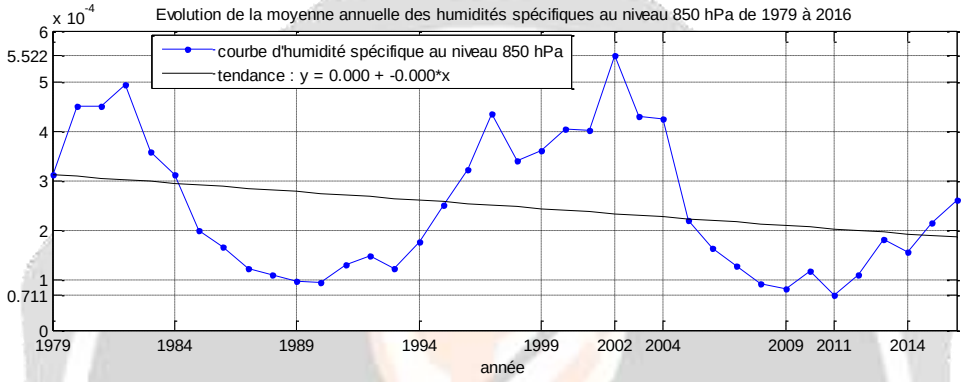

Figure 3-b

Figure 3 : curves and trend lines of specific humidities annual mean

3.3 Annual anomaly of specific humidity on 700 hPa level from 1979 to 2016

Figure 4 shows annual anomalies for specific humidities at the 700 hPa and 850 hPa levels.
The study period is marked by an almost alternating period of excess and deficiency specific humidity on the 700 hPa level. The maximum value ($3.7x10^{-4}$ $kg.kg^{-1}$) was observed in 1997 and the minimum value ($2.47x10^{-4}$ $kg.kg^{-1}$) in 1986. Very close to minimum values were observed in 1992, 2008 and 2015. (**Figure 4-a)**
During the study period, the specific humidity at the 850 hPa level is generally in deficit, characterized by a negative annual anomaly. However, there were two very marked positive anomalies in 1980 ($2.81x10^{-3}$ $kg.kg^{-1}$) and 1984 ($2.47x10^{-3}$ $kg.kg^{-1}$). (**Figure 4-b**).

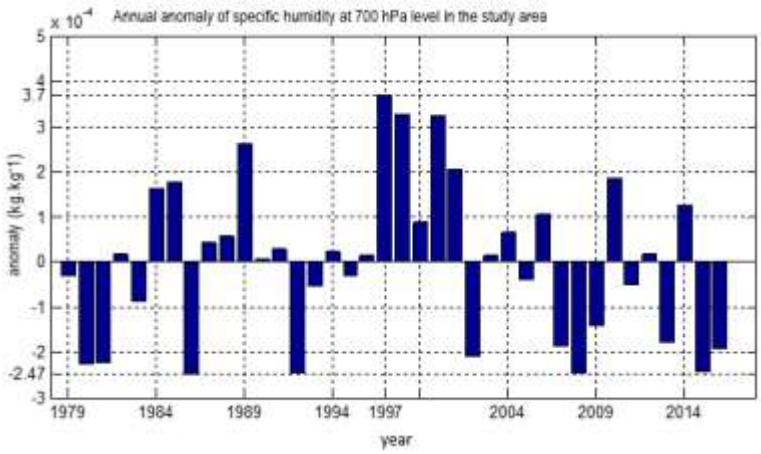

Figure 4-a : annual anomaly of specific humidity on 700 hPa level

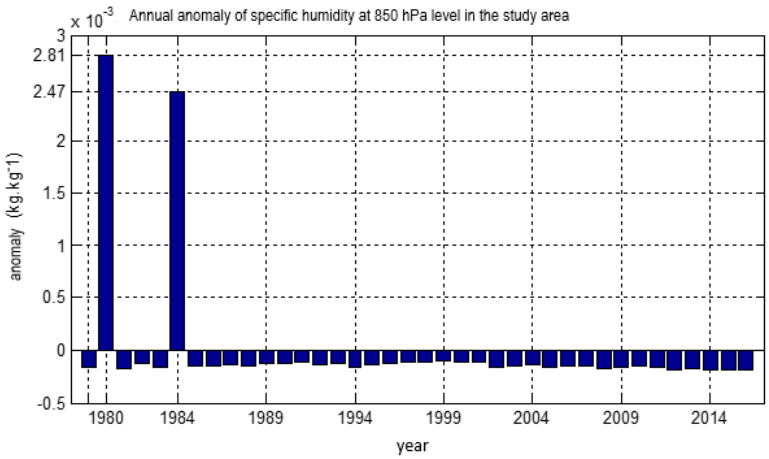

Figure 4-b : annual anomaly of specific humidity on 850 hPa level

Figure 4 : annual anomaly of specific humidities from 1979 to 2016

3.4 Principal Components Analysis results

In the Principal Components Analysis study, all the specific humidities of each point of intersection of latitude and longitude were selected as individuals in the study area following the spatial resolution of 1° x 1° and as variables the 12 months of the year. Which gives 5 rows according to the latitude and 4 rows according to the longitude. There are therefore 20 intersecting points representing individuals. (**Figure 5**)

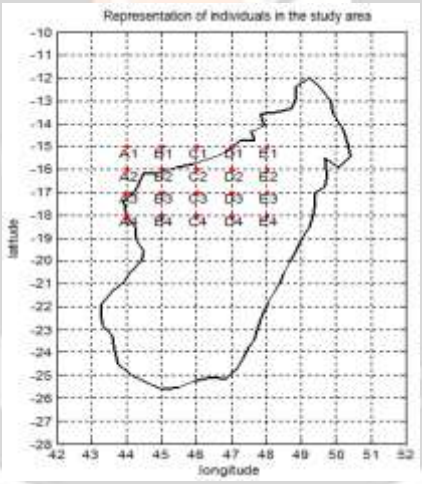

Figure 5 : representation of individuals in the study area

3.4.1 Choice of number of axes to choose

To study the behaviour of each individual vis-à-vis others, the Kaiser criterion and the elbow criterion allow to keep the factorial axes F1 and F2. These two axes explain 92.64% of the total inertia cloud for specific humidity on700 hPa level (**Figure 6-a**) and 90.13% for specific humidity on 850 hPa level (**Figure 6-b**).

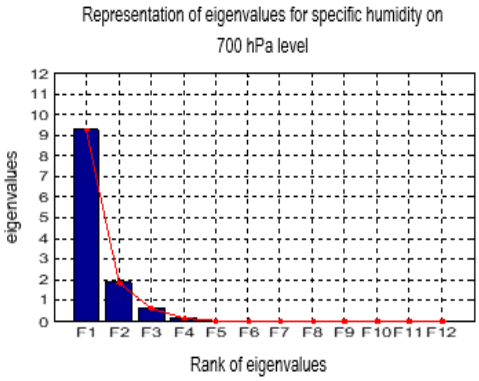

Figure 6-a

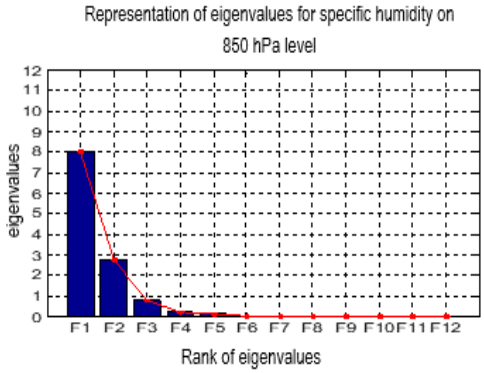

Figure 6-b

Figure 6 : representation of specific humidity eigenvalues

3.4.2 Projections of variables on the factorial plane F1-F2

Figure 7 shows the projection of variables in the factorial plane F1-F2.

- Months of low specific humidity on 700 hPa level are generally well represented in the plane F1-F2. These months are positively correlated with the axis F1 which explains 77.11% of the total inertia of the scatter plot. The axis F1 therefore represents the dry months. (**Figure 7-a**)
- Les mois d'octobre et novembre sont corrélés positivement avec l'axe F2 contrairement aux mois de janvier et février. L'axe F2 oppose les mois très humides en été austral aux mois moyennement humide à la fin d'hiver et début d'été austraux. (**Figure 7-a)**
- October and November are positively correlated with the F2 axis unlike January and February. The axis F2 contrasts the very humid months in the southern summer with the moderately humid months in the late winter and early summer. (**Figure 7-a**)
- Every month is very well represented in the factorial plan F1-F2 for specific humidity at 850 hPa level, except for June, October and November. The humid months are positively correlated with the F1 axis which explains 67.11% of the total inertia of the scatter plot, and the dry months negatively. As a first approximation, the axis F1 orders the months according to their increasing humidity. (**Figure 7-b**)

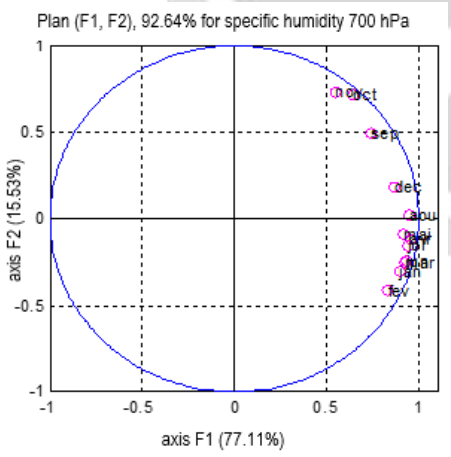

Figure 7-a

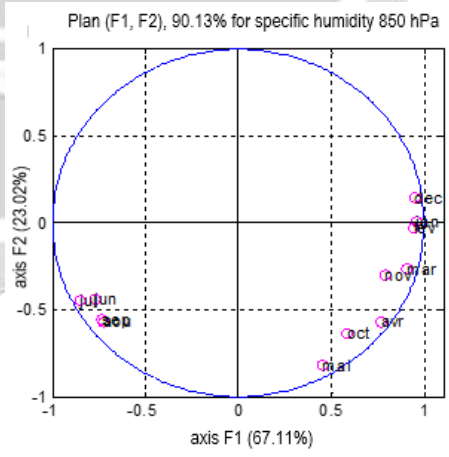

Figure 7-b

Figure 7 : projection of variables on the factor plane F1-F2 for specific humidities on 700 hPa and 850 hPa levels

3.4.3 Projections of individuals

Figure 8 shows the projection of individuals in the factorial plane F1-F2.

In **Figure 8-a**, for the specific humidity on 700 hPa level :

- the individual A4 contributes the most to the construction of the F1 axis. This individual is of low specific humidity in austral winter considering correlation of the variables with axis F1. It is the same for individuals in its category.
- The individual A1 could be in the same category as A4 during the austral winter but in addition it is moderately humid at the end of winter and at the beginning of summer austral according to the correlation of the variables with the axis F2 .
- the axis F1 opposes the individual E3 to A4. The E3 individual is wetter in the austral winter than the individual A4. It is the same for individuals in the same category as E3.
- the individual E1 contributes the most to the construction of the axis F2. This individual is moderately wet at the end of winter and at the beginning of summer austral seen its coordinate with respect to the axis F2 and according to the correlation of the variables with this axis. Individuals in its category adopt this same behavior in the austral spring.
- the axis F2 opposes the individual B3 to E1. This individual is of high humidity in austral summer. Same for individuals in its category.

In **Figure 8-b**, for specific humidity at the 850 hPa level :

- the individual A4 contributes the most to the formation of the F1 axis. According to the correlation of the variables with the axis F1, this individual is of high humidity in austral summer. It is the same for individuals in its category.
- the axis F1 opposes the individual E1 to A4. The E1 individual is of very low humidity in the austral winter as the A4 individual. It is the same for individuals in the same category as E1.

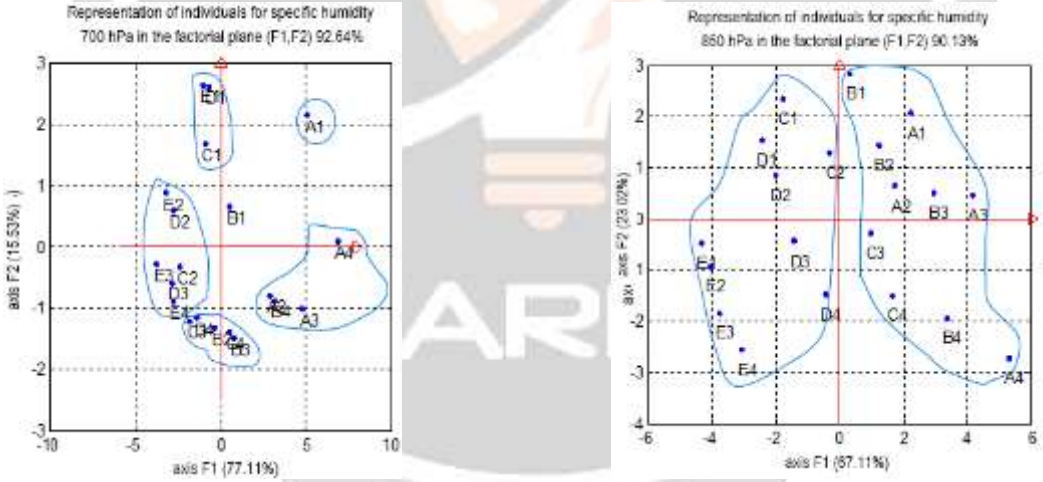

Figure 8-a **Figure 8-b**

Figure 8 : projection of individuals on the factor plane F1-F2 for specific humidities on 700 hPa and 850 hPa levels

3.4.4 Regionalization of the study area

Based on the results of individual and variables projections on the factorial plane (F, F2), the study area can be subdivided : **(Figure 9)**

- in 5 regions for specific humidity on 700 hPa level :

région 1 : consisting of A1 (in sky blue).This region is low specific humidity in the southern winter and medium humidity in the southern spring.

région 2 : consisting of **A2**, **A3**, **A4**, and **B4** (in blue). This region is of low specific humidity in austral winter.

région 3 : consisting of **E1, C1** and **D1** (in green). This area is moderately wet in late winter and early summer.

région 4 : consisting of **C2**, **C3**, **D2**, **D3**, **E2**, **E3** and **E4** (in purple). This region is of relatively high humidity in the austral winter.

région 5 : consisting of **B2**, **B3**, **C4** and **D4** (in red). This region is of high humidity in austral summer.

- in 2 regions for the specific humidity on 850 hPa level :

région 1 : consisting of **A1**, **A2**, **A3**, **A4**, **B1**, **B2**, **B3**, **B4** , **C3** and **C4** (in red). This region is characterized by high humidity in austral summer.

région 2 : consisting of **C1**, **C2**, **D1**, **D2**, **D3**, **D4**, **E1**, **E2**, **E3** and **E4** (in blue). This region has very low humidity in southern winter than region 1.

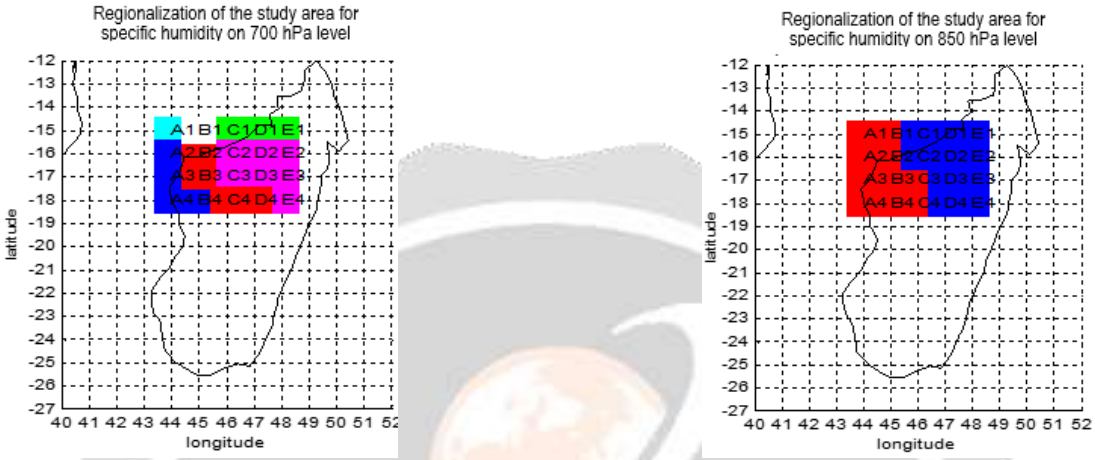

Figure 9 : distribution of regions with similar specific humidities on 700 hPa and 850 hPa levels

3.5 Bias correction of the MOHC HadGEM2-CC climate model under the scenarios RCP4.5 and RCP8.5

3.5.1 Correction of specific humidity bias on 700 hPa level and choice of suitable method

The most suitable method of correction is the one whose average difference between its result and the observation is minimal in absolute value.

- **Figure 10** shows the bias corrections of the MOHC HadGEM2-CC climate model under RCP4.5 scenarios of the specific humidity on 700 hPa level, in regions 1 to 5, by the debinding method, the delta method and the quantile-quantile method.

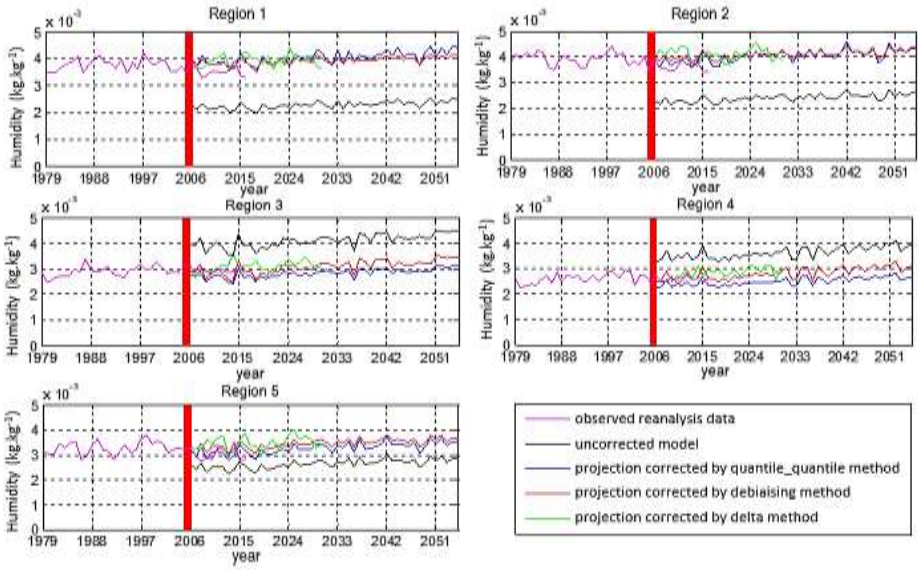

Figure 10 : Correction of MOHC HadGEM2-CC climate model under the RCP4.5 scenario for specific humidity on 700 hPa level

Table 1 summarizes the average difference between the result of each correction method and the observation over the validation period 2006-2016. This **Table 1** shows the best method for each region.

Table 1 : average difference between the result of each correction method and the observation

Regions	**Mean differences with observation (in kg.kg^{-1}) over the validation period 2006-2016**			**Adapted correction method**
	quantile-quantile	**debinding**	**delta**	
Region 1	-2,9533x10^{-5}	**-2,6034x10^{-5}**	-3,3682x10^{-5}	Debinding method
Region 2	**-1,4605x10^{-5}**	-2,7532 x10^{-5}	-4,0431x10^{-5}	Quantile-quantile method
Region 3	2,5119x10^{-5}	7,7372x10^{-6}	**-4,8467x10^{-6}**	Delta method
Region 4	1,4501e-05	**-1,0916x10^{-5}**	-1,5684e-05	Debinding method
Region 5	**-6,0333x10^{-6}**	-2,6464 x10^{-5}	-3,7206 x10^{-5}	Quantile-quantile method

- **Figure 11** shows the bias corrections of the MOHC HadGEM2-CC climate model under RCP8.5 scenarios of the specific humidity on 700 hPa level, in regions 1 to 5, by the debinding method, the delta method and the quantile-quantile method.

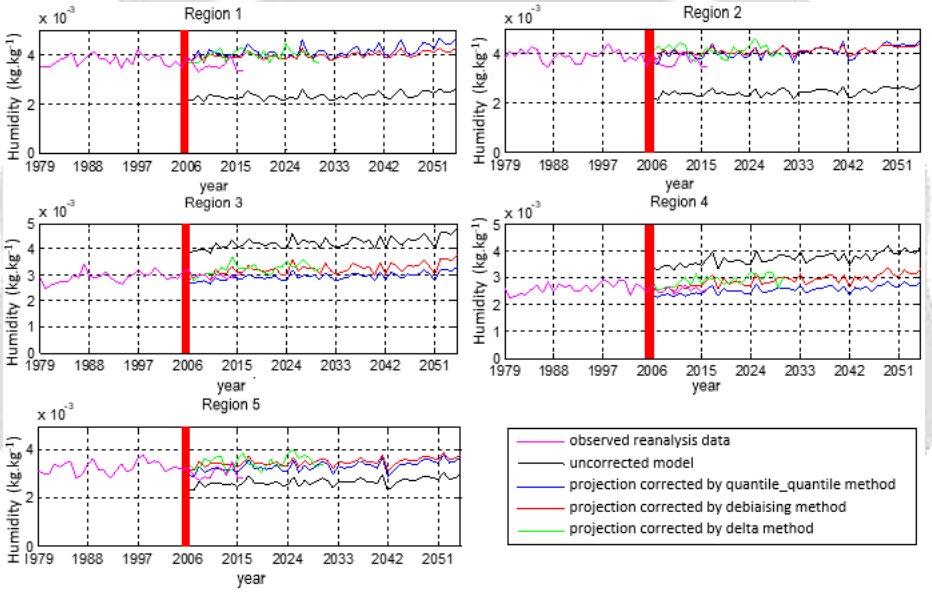

Figure 11 : correction of MOHC HadGEM2-CC climate model under the RCP8.5 scenario for specific humidity on 700 hPa level

Table 2 summarizes the average difference between the result of each correction method and the observation during the 2006-2016 validation period. **Table 2** shows the best method for each region.

Table 2 : average difference between the result of each correction method and the observation

Regions	**Mean differences with observation (in kg.kg^{-1}) over the validation period 2006-2016**			**Adapted correction method**
	quantile-quantile	**debinding**	**delta**	
Region 1	-3.8662x10^{-5}	**-3.1178x10^{-5}**	-3.7459x10^{-5}	Debinding method
Region 2	**-2.1503x10^{-5}**	-3.1649x10^{-5}	-4.2320x10^{-5}	Quantile-quantile method
Region 3	1.6618x10^{-5}	**-4.5653x10^{-6}**	-1.6939x10^{-5}	Debinding method
Region 4	1.6335x10^{-5}	**-8.2484x10^{-6}**	-2.2656x10^{-5}	Debinding method
Region 5	**-1.0902x10^{-5}**	-3.0384x10^{-5}	-4.0563x10^{-5}	Quantile-quantile method

3.5.2 Correction of specific humidity bias on 850 hPa level and choice of suitable method

- **Figure 12** shows the bias corrections of the MOHC HadGEM2-CC climate model under RCP4.5 scenarios of the specific humidity on 850 hPa level, in regions 1 and 2, by the debinding method, the delta method and the quantile-quantile method.

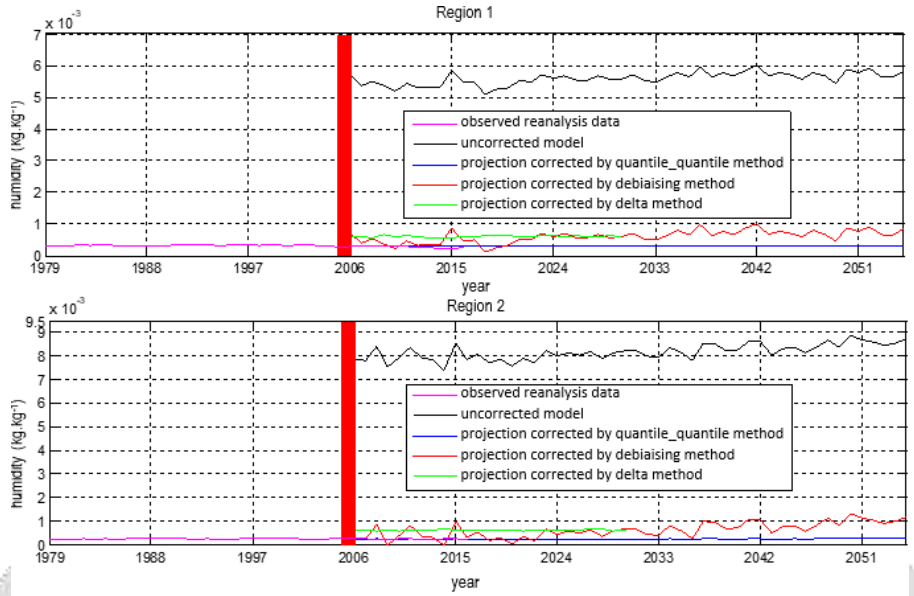

Figure 12 : correction of MOHC HadGEM2-CC climate model under the RCP4.5 scenario for specific humidity on 700 hPa level

Table 3 summarizes the average difference between the result of each correction method and the observation during the 2006-2016 validation period. **Table 3** shows which of these methods is best suited for each region.

Table 3 : average difference between the result of each correction method and the observation

Regions	**Mean differences with observation (in kg.kg^{-1}) over the validation period 2006-2016**			**Adapted correction method**
	quantile-quantile	**debinding**	**delta**	
Region 1	**1.1839x10^{-6}**	-1.5817x10^{-5}	-3.4284x10^{-5}	Quantile-quantile method
Region 2	**-2.4065x10^{-6}**	-1.6746x10^{-5}	-2.9577x10^{-5}	Quantile-quantile method

- **Figure 13** shows the bias corrections of the MOHC HadGEM2-CC climate model under RCP8.5 scenarios of the specific humidity on 850 hPa level, in regions 1 and 2, by the debinding method, the delta method and the quantile-quantile method.

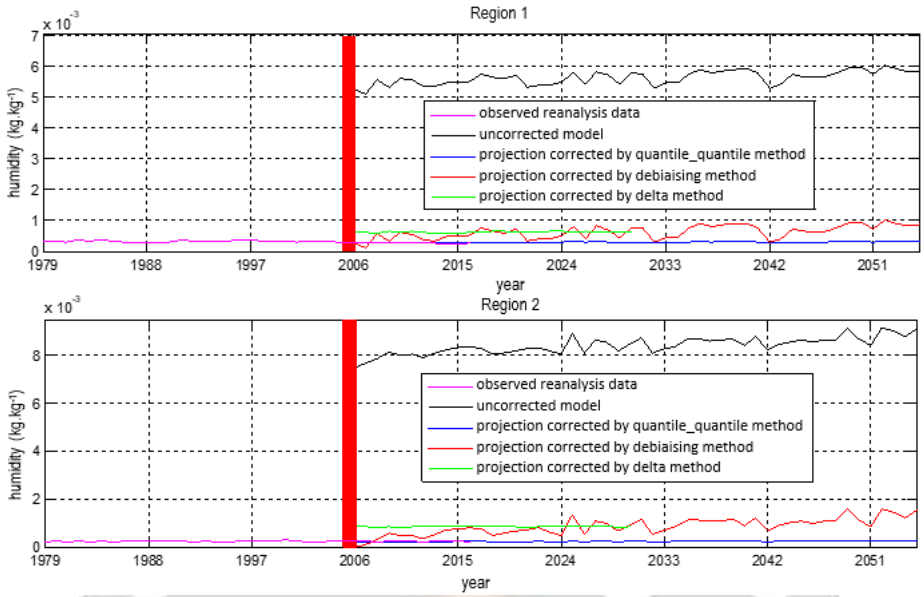

Figure 13 : Correction of MOHC HadGEM2-CC climate model under the RCP8.5 scenario for specific humidity on 850 hPa level

Table 4 summarizes the average difference between the result of each correction method and the observation over the 2006-2016 validation period. **Table 4** shows the most suitable method for each of these regions.

Table 4 : average difference between the result of each correction method and the observation

Regions	**Mean differences with observation (in kg.kg^{-1}) over the validation period 2006-2016**			**Adapted correction method**
	quantile-quantile	**debinding**	**delta**	
Region 1	**-2.2275x10^{-6}**	-1.3500x10^{-5}	-3.1047x10^{-5}	Quantile-quantile method
Region 2	**1.0085x10^{-6}**	-2.1017x10^{-5}	-5.5810x10^{-5}	Quantile-quantile method

4. CONCLUSIONS

In this article, we conducted the study of specific humidity followed by bias correction of the HadGEM2-CC climate model of the Met Office Hadley Center (MOHC) in the northwest region of Madagascar, delimited by latitudes -15 ° to -18 ° and longitudes 44 ° to 48°. The validation of the study is made over the period 2006-2016 by referring to the data of reanalysis of specific humidity on 700 hPa and 850 hPa levels resulting from NOAA during the period 1979 -2016.

The study of evolution of annual mean specific humidities on 700 hPa and 850 hPa levels showed the absence of significant trend according to the Mann Kendall test.

The result of the Principal Component Analysis showed the existence of :

- five regions with the same climatic conditions for specific humidity on 700 hPa:

region 1 : it is a region of specific low humidity in the southern winter and medium humidity in the southern spring.
region 2 : this region is of low specific humidity in the southern winter.
region 3 : this region is moderately humid in late winter and early southern summer.
region 4 : it is a relatively high humidity region in the southern winter.
region 5 : this region is marked by high humidity in the southern summer.

- two regions with the same climatic conditions for specific humidity on 850 hPa level :

region 1 : this region is characterized by high humidity in austral summer.
region 2 : this region has very low humidity in southern winter compared to region 1.

We conducted the bias correction of the HadGEM2-CC Met Office Hadley Center climate model under scenarios RCP4.5 and RCP8.5 in each region :

- the model bias correction for specific humidity on 700 hPa level showed that :

➢ the debinding method is suitable for:
- region 1 and region 4 under the RCP4.5 scenario ;
- region 1, region 3 and region 4 under the RCP8.5 scenario;

➢ the quantile-quantile method is suitable for :
- region 2 and region 5 under the RCP4.5 scenario;
- region 2 and region 5 under the RCP8.5 scenario;

➢ the delta method is suitable for region 3.

- the model bias correction for specific humidity on 850 hPa level has shown that the quantile-quantile method is suitable for both regions (region 1 and region 2) under both RCP4.5 and RCP8.5 .

5. REFERENCES

[1] N. Croiset, B. Lopez (BRGM), Outil d'analyse statistique des séries temporelles d'évolution de la qualité des eaux souterraines, Manuel d'utilisation, Rapport final, pp.18-19

[2] P. Besse www.math. univ-toulouse.fr/besse, M2 MASS, TP4 : Introduction au logiciel SAS Procédures statistiques multivariées : Analyse en Composantes Principales. Pages 1, 2.

[3] C.DUBY, S ROBIN ; Analyse composantes principale, juillet 2006. Pages 4,5.

[4] Aimé KOUDOU et al, CONTRIBUTION DE L'ANALYSE EN COMPOSANTES PRINCIPALES A LA REGIONALISATION DES PLUIES DU BASSIN VERSANT DU N'ZI, CENTRE DE LA COTE D'IVOIRE, 2015. Page 162.

[5] Ali Kouani, S. El Jamali et M.Talbi, Analyse en Composantes principales, Une méthode factorielle pour traiter les données didactique, février 2007. Page 3.

[6] ADD3-MAB, D-interpretation d'une ACP, 2011.Papes 4, 29.

[7] Jean-Marc Labatte, jean-marc.Labatte@univ-angers.fr, Analyse des données M2, consulté le 17 Février 2017.

[8] Tanina. D. SORO, Nagnin SORO, 2011: Variabilité climatique et son impact sur les ressources en eau dans le dégré carrré de grand-lahou (Sud-Ouest de la cote d'ivoire). Pages 125, 131.

[9] Julien Boé : Désagrégation spatiale : les différentes approches avec des applications dans l'étude des impacts du changement climatique, 26 Septembre 2014. Page 25.

[10] Frédéric HUARD, INRA Agro Clim, Régionalisation statistique pour les études d'impact du changement climatique : pourquoi et comment. Pages 7, 8, 9, 10